

A Simplified Geometric Channel Model for Mobile-to-Mobile Communications

Konstantinos B. BALTZIS

RadioCommunications Laboratory, Dept. of Physics, Aristotle University of Thessaloniki, Greece

kmpal@physics.auth.gr

Abstract. *In Mobile-to-Mobile (M2M) communications, the communicating nodes are surrounded by scatterers and equipped with low elevation antennas. This paper proposes a simple 2-D geometric scattering model for M2M channels. The model is also applicable in cellular systems when we employ low height base station antennas. In our approach, the scatterers are uniformly distributed in ellipses with arbitrary size and orientation around each communicating node. We provide simple formulas for the calculation of the angular spread and delay variation of the propagating signal. Simulation results verify the accuracy of the model. In order to validate the generalization of the approach, we compare it against notable models in the literature. As an application example, we investigate the impact of scatterer distribution and separation between mobiles on the angle and time of arrival statistics of the multipaths.*

Keywords

Angle of arrival, time of arrival, regular-shaped Geometrical-Based Stochastic Models, scattering, Mobile-to-Mobile channel.

1. Introduction

In the last decade, M2M communications have received special attention mainly due to their applications in intelligent transportation systems, relay-based cellular networks and vehicular networking [1]. M2M communication systems differ from cellular ones in several points. Contrary to cellular networks, in M2M systems both transmitter and receiver are in motion and equipped with low height antennas. Also, the physical environment is highly dynamic, that is, the propagation channel is non-stationary. Obviously, engineers should address several challenges prior to the wide development of these systems. A new level of understanding of the characteristics of the propagation medium is also required [2], [3].

In recent years, intensive studies have been carried out to describe the complicated nature of the M2M channel. A common classification of the existing models is

based on the modeling of the environment and the distribution of objects within it. Generally, we classify M2M channel models into the deterministic and the stochastic ones; the latter are further divided into Non-Geometrical Stochastic Models (NGSMs) and Geometrical-Based Stochastic Models (GBSMs) [4], [5].

Deterministic models [6], [7] mainly use ray tracing techniques [8], [9]. They show close agreement with measured data and are easily reproducible but at the expense of high computational complexity; they also require detailed knowledge of the geometry and the physical properties of the propagation medium. The model in [6] considers both static and mobile objects in the environment and evaluates channel characteristics by analyzing the strongest transmission paths between the communicating nodes. The authors in [7] modeled the road traffic, the environment adjacent to the road lane and the wave propagation between the mobiles and obtained results consistent with narrow-band and wide-band channel measurements at 5.2 GHz.

NGSMs are usually empirical approaches that determine channel physical parameters in a stochastic manner. The origin of the model standardized by the M2M communications standard 802.11p is a single-input single-output model that calculates channel statistics without presuming any underlying geometry [10]. Extensive measurement campaigns indicated specific features of M2M communication channels and their strong dependence on traffic characteristics allowing the derivation of channel models for various environments and given traffic density values [1], [11], [12].

On the other hand, geometric modeling idealizes the wireless channel via a geometric abstraction of the spatial relationships among the communicating nodes and the scatterers. Geometric models usually target to the computation of the angle of arrival (AoA) and time of arrival (ToA) statistics of the received signal [13]. Their simplicity and reduced computational cost make them the most popular M2M channel models [14] despite that they usually fail to describe the non-stationary character of the medium because they assume static effective scatterers located on regular geometric shapes [15]-[18].

In this paper, we propose a simple 2-D GBSM for the M2M channel. Needless to say, two-dimensional modeling

neglects signal variation in the elevation plane [19]. However, in M2M systems the antennas height is low allowing us to ignore the elevation angular spread of the propagating signal. Our approach extends [15] by considering scatterers uniformly distributed within ellipses (instead of circles) that provides a better description of the channel. The proposed model can also be viewed as a generalization of two popular channel models for cellular systems [20], [21]. We provide simple expressions for the AoA probability density function (pdf) and ToA cumulative distribution function (cdf) of the incoming multipaths at the mobiles' antennas. Comparisons with simulation results and models in the literature validate and generalize our method. Finally, we explore the impact of scatterer distribution on the angular and temporal spread of the received multipaths. It has to be noticed that a number of models in the literature describe more accurately the M2M channel. However, the simplicity of the proposal and the description of AoA and ToA statistics with easily reproducible expressions provide a better physical insight of the channel and reduce significantly the computational requirements of link- and system-level simulations of M2M communication systems.

The rest of the paper is organized as follows: Section 2 presents the system model and assumptions. In Section 3, we derive the AoA pdf and ToA cdf expressions. Next, in Section 4, we validate the formulation and generalize its application through comparisons with simulation results and models in the literature. Section 5 presents examples that explore the impact of channel parameters on the spatial and temporal characteristics of the propagating signal. Finally, Section 6 concludes this work.

2. System Model and Assumptions

We consider two mobiles M_1 and M_2 placed at $(0,0)$ and $(D,0)$ (in the Cartesian coordinates system). Each mobile is surrounded by scatterers uniformly distributed within ellipses, we call them "scattering ellipses", with semi-major axes $a_{1,2}$ and semi-minor axes $b_{1,2}$, centered at M_1 and M_2 . Finally, the angles between $a_{1,2}$ and the x -axis are $\Phi_{1,2} \in [0, \pi]$, see Fig. 1.

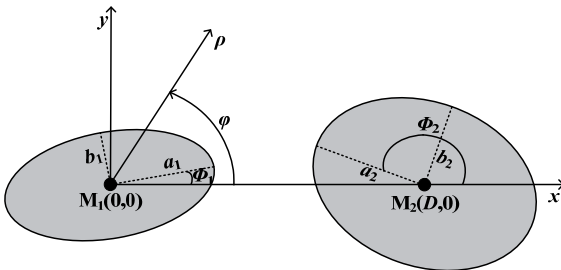


Fig. 1. The proposed M2M channel model.

In order to develop our model, we assume that the mobiles are equipped with low height antennas and move at low speed, assumptions that allow the description of the channel with a 2-D stationary model [22]. Other common geometric modeling assumptions that we made are:

- Multipaths undergo a single-bounce travelling from the transmitter to the receiver and reach the receiver antenna at the same power level without phase difference among them.
- The effective radiation patterns of the mobiles' antennas are omni-directional.
- Scatterers have equal scattering coefficients with uniform random phases and act as independent omni-directional lossless reradiating elements.
- Polarization effects are negligible.

3. AoA/ToA Statistics: Mathematical Formulation

In this section, we develop the mathematical framework for the description of the AoA and ToA statistics of the incoming multipaths at the mobiles' antennas. In particular, we provide a closed-form expression for the AoA pdf $f_\phi(\phi)$ and a simple integral formula for the ToA cdf $F_\tau(\tau)$.

3.1 Angle-of-Arrival Statistics

Let us consider an ellipse centered at (X_0, Y_0) with semi-major axis a rotated by an angle Φ relative to the x -axis and semi-minor axis b . We can easily show that the expression of this ellipse in polar coordinates is the quadratic formula

$$\left(\frac{\cos^2 \phi'}{a^2} + \frac{\sin^2 \phi'}{b^2}\right) \rho^2 - 2\left(\frac{X' \cos \phi'}{a^2} + \frac{Y' \sin \phi'}{b^2}\right) \rho + \left(\frac{X'}{a}\right)^2 + \left(\frac{Y'}{b}\right)^2 - 1 = 0 \quad (1)$$

with solutions

$$\rho^\pm(\phi) = \frac{1}{a^2 \sin^2 \phi' + b^2 \cos^2 \phi'} \left(b^2 X' \cos \phi' + a^2 Y' \sin \phi' \pm ab \sqrt{a^2 \sin^2 \phi' + b^2 \cos^2 \phi' - (X' \sin \phi' - Y' \cos \phi')^2} \right) \quad (2)$$

where $X' = X_0 \cos \Phi + Y_0 \sin \Phi$, $Y' = -X_0 \sin \Phi + Y_0 \cos \Phi$ and $\phi' = \phi - \Phi$.

As a result, the scattering ellipses around M_1 and M_2 are respectively described from the expressions

$$\rho_1(\phi) = \frac{a_1 b_1}{\sqrt{a_1^2 \sin^2(\phi - \Phi_1) + b_1^2 \cos^2(\phi - \Phi_1)}}, \quad \phi \in [-\pi, \pi] \quad (3)$$

and

$$\rho_2^\pm(\phi) = \begin{cases} \frac{1}{a_2^2 \sin^2(\phi - \Phi_2) + b_2^2 \cos^2(\phi - \Phi_2)} \\ \times [D(b_2^2 \cos(\phi - \Phi_2) \cos \Phi_2 \\ - a_2^2 \sin(\phi - \Phi_2) \sin \Phi_2) \\ \pm a_2 b_2 (a_2^2 \sin^2(\phi - \Phi_2) \\ + b_2^2 \cos^2(\phi - \Phi_2) - D^2 \sin^2 \phi)^{1/2}] \\ 0, \end{cases} \quad \phi \in [\varphi^-, \varphi^+] \quad (4)$$

with φ^\pm the solutions of $\rho_2^+(\varphi) = \rho_2^-(\varphi)$ calculated as

$$\begin{aligned} \varphi^\pm = \operatorname{atan} & \left(\frac{1}{a_2^2 \cos^2 \Phi_2 + b_2^2 \sin^2 \Phi_2 - D^2} \right. \\ & \times \left[(a_2^2 - b_2^2) \cos \Phi_2 \sin \Phi_2 \right. \\ & \left. \mp \sqrt{D^2 (a_2^2 \sin^2 \Phi_2 + b_2^2 \cos^2 \Phi_2) - a_2^2 b_2^2} \right] \end{aligned} \quad (5)$$

In our model, the scatterers are uniformly distributed within the scattering ellipses. Therefore, the area of the intersection of these regions with the triangle with tip at $(0,0)$ and sides the rays that emanate from $(0,0)$ at angles φ and $\varphi + \Delta\varphi$ with $\Delta\varphi \ll \varphi$ (shaded area, see Fig. 2) is proportional to the probability of the AoA of the multipaths at M_1 . Obviously, the area of the intersection of this triangle and the ellipse at site M_1 is $A_1(\varphi) \approx \rho_1^+(\varphi) \Delta\varphi/2$ while the area of the intersection of the triangle and the second ellipse is $A_2(\varphi) \approx [(\rho_2^+(\varphi))^2 - (\rho_2^-(\varphi))^2] \Delta\varphi/2$.

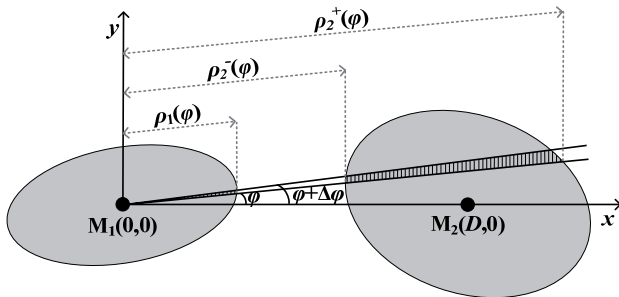


Fig. 2. Calculation of the AoA probability at M_1 site.

Based on the above, the cdf of the AoA of the received signal at M_1 is obtained from the ratio of the integral of the quantity $A_1(\varphi) + A_2(\varphi)$ over φ to the area of the two scattering ellipses; differentiation of this cdf with respect to φ gives the AoA pdf at M_1 , that is,

$$f_\varphi(\varphi) = \frac{\rho_1^2(\varphi) + (\rho_2^+(\varphi))^2 - (\rho_2^-(\varphi))^2}{2\pi(a_1b_1 + a_2b_2)}. \quad (6)$$

In this analysis, we assumed the same scatterer density in the scattering ellipses; if this is not a case, and set σ the ratio of the scatterer density around M_2 to the scatterer density around M_1 (relative scatterer density), we easily obtain as in [15] the more general formula

$$f_\varphi(\varphi) = \frac{\rho_1^2(\varphi) + \sigma [(\rho_2^+(\varphi))^2 - (\rho_2^-(\varphi))^2]}{2\pi(a_1b_1 + \sigma a_2b_2)}. \quad (7)$$

Obviously, the AoA pdf at M_2 is derived by simply interchanging indices “1” and “2” in (6) or (7).

3.2 Time-of-Arrival Statistics

In order to calculate the ToA statistics, we set the coordinates origin at the midpoint between M_1 and M_2 and consider an ellipse, we call it “bounding ellipse”, centered at $(0,0)$ with axes $c\tau$ and $\sqrt{c^2\tau^2 - D^2}$, where τ is the time

delay and c is the speed of light. In this case, all the scatterers responsible for contribution towards a certain time delay (or equivalently, time of arrival) τ are located on the circumference of this ellipse [15], [21], [23]. In order to simplify the analysis, we also assume that the scattering ellipse at M_1 (M_2) site is restricted to $x \leq 0$ ($x \geq 0$).

Using (1), we obtain the expressions of the bounding ellipse

$$\rho_{0,\tau}(\varphi) = \frac{c\tau}{2} \sqrt{\frac{c^2\tau^2 - D^2}{c^2\tau^2 - D^2 \cos^2 \varphi}}, \quad \varphi \in [-\pi, \pi] \quad (8)$$

and the scattering ellipse around M_1

$$\rho_{1,\tau}^\pm(\varphi) = \begin{cases} \frac{1}{a_1^2 \sin^2(\varphi + \Phi_1) + b_1^2 \cos^2(\varphi + \Phi_1)} \\ \times \left[-\frac{D}{2} (b_1^2 \cos(\varphi + \Phi_1) \cos \Phi_1 \right. \\ \left. + a_1^2 \sin(\varphi + \Phi_1) \sin \Phi_1) \right. \\ \left. \pm a_1 b_1 (a_1^2 \sin^2(\varphi + \Phi_1) \right. \\ \left. + b_1^2 \cos^2(\varphi + \Phi_1) - \frac{D^2}{4} \sin^2 \varphi) \right]^{1/2} \\ 0, \end{cases} \quad \varphi \notin [\varphi_1^-, \varphi_1^+] \quad (9)$$

$$\varphi \in [\varphi_1^-, \varphi_1^+] \quad (9)$$

with φ_1^\pm the solution of $\rho_{1,\tau}^+(\varphi) = \rho_{1,\tau}^-(\varphi)$ given by

$$\begin{aligned} \varphi_1^\pm = \pm\pi - \operatorname{atan} & \left(\frac{1}{a_1^2 \cos^2 \Phi_1 + b_1^2 \sin^2 \Phi_1 - \frac{D^2}{4}} \right. \\ & \times \left[(a_1^2 - b_1^2) \cos \Phi_1 \sin \Phi_1 \right. \\ & \left. \mp \sqrt{\frac{D^2}{4} (a_1^2 \sin^2 \Phi_1 + b_1^2 \cos^2 \Phi_1) - a_1^2 b_1^2} \right] \end{aligned} \quad (10)$$

The expression of the scattering ellipse around M_2 $\rho_{2,\tau}^\pm(\varphi)$ is directly obtained from (4) by replacing D with $D/2$. This replacement is also applied in (5) and gives the angles φ_2^\pm that define the range in which $\rho_{2,\tau}^\pm(\varphi) \neq 0$.

The ToA cdf equals to the probability that a scatterer is placed inside the bounding ellipse corresponding to a delay τ . Therefore, and due to the uniform scatterer distribution, it is calculated from the ratio of the area of overlap of the bounding and each of the scattering ellipses (darker region in Fig. 3) to the area of the scattering region.

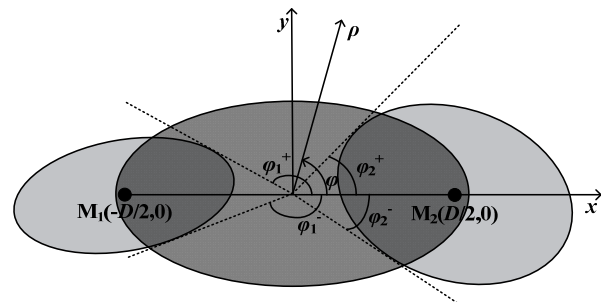


Fig. 3. Calculation of the ToA probability.

As a result the ToA cdf is given by

$$F_{\tau}(\tau) = \frac{\int_{-\pi}^{\varphi_1^-} R_1(\varphi) d\varphi + \int_{\varphi_1^+}^{\pi} R_1(\varphi) d\varphi + \sigma \int_{\varphi_2^-}^{\varphi_2^+} R_2(\varphi) d\varphi}{2\pi(a_1 b_1 + \sigma a_2 b_2)} \quad (11)$$

with

$$R_{1(2)}(\varphi) = \left(\left[\min(\rho_{0,\tau}(\varphi), \rho_{1(2),\tau}^+(\varphi)) \right]^2 - \left[\rho_{1(2),\tau}^-(\varphi) \right]^2 \right) \times u(\rho_{0,\tau}(\varphi) - \rho_{1(2),\tau}^-(\varphi)) \quad (12)$$

where $u(\cdot)$ denotes the unit step function.

The ToA pdf is obtained from the numerical differentiation of $F_{\tau}(\tau)$ with respect to τ . Obviously, the ToA statistics at M_1 and M_2 are the same since the distance travelled by a multipath between the mobiles is independent of the direction (uplink-downlink symmetry) [21], [24].

4. Model Validation

In this section, we validate our model through comparisons with simulation results and models in the literature. We performed several simulations for different channel scenarios. The results for a representative case follows; in this example, system parameters are: $\sigma^0 = 0.5$, $D^0 = 100\text{m}$, $a_1^0 = 30\text{m}$, $b_1^0 = 20\text{m}$, $a_2^0 = 20\text{m}$, $b_2^0 = 15\text{m}$, $\Phi_1^0 = 45\text{deg}$ and $\Phi_2^0 = 20\text{deg}$.

Fig. 4 illustrates the scatterers' positions for 10^4 snapshots; clearly, scatterer density is higher around M_1 . Next, Figs. 5 and 6 plot the curves obtained from (7) and (11), respectively, and the simulated AoA pdf and ToA cdf for 10^5 snapshots. In both cases, we observe an excellent agreement between simulation results and analytical curves.

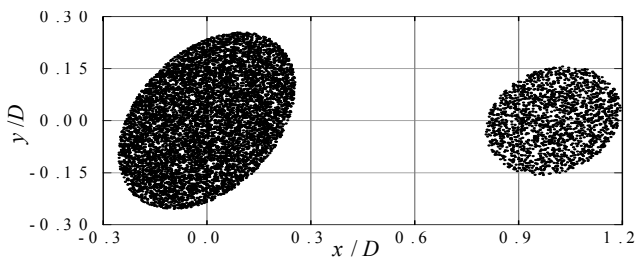


Fig. 4. Spatial distribution of scatterers.

In order to further validate and demonstrate the generalization of our approach, we compare it with notable 2-D geometric models [15], [20], [21]. The authors in [15] presented a geometric model for the M2M channel assuming scatterers uniformly distributed in two circular disks centered at the mobiles. In [20] and [21], scatterers were uniformly distributed around an ellipse or a circle, respectively, centered at the transmitter while the receiver was outside the scattering area. It easily comes that the three models are derived from the proposed one by setting $a_1=b_1$,

$a_2=b_2$ in the first, $a_1=b_1=\Phi_2=0$ in the second and $a_2=b_2$, $a_1=b_1=0$, in the third case.

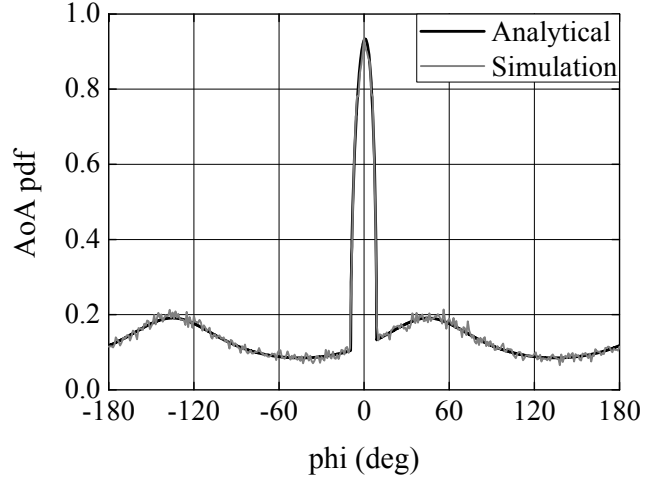


Fig. 5. Simulation results and analytical AoA pdf curve.

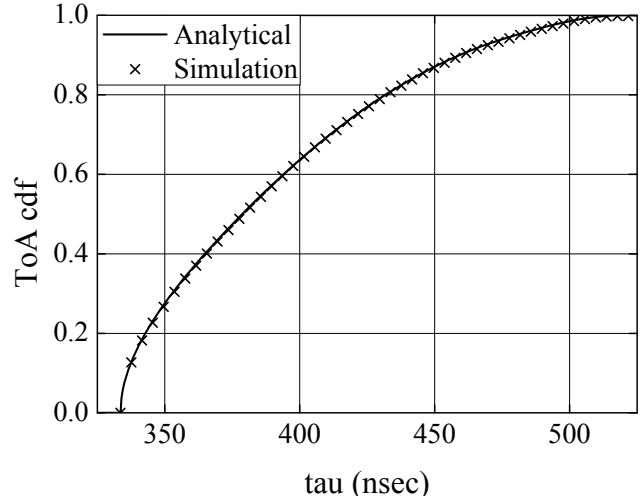


Fig. 6. Simulation results and analytical ToA cdf curve.

5. Numerical Examples and Discussion

In this section, we provide illustrative examples and explore the impact of channel parameters on the spatial distribution and the delay variation of the received signal. The initial values of the parameters were set in the previous section. In each example, we vary one parameter at a time and hold the rest at their initial values. All the results have been verified through simulations. In the following examples, we plot the pdf curves so as to provide a better illustration of the impact of channel parameters on signal statistics. In this work, we calculate the ToA pdf as

$$f_{\tau}(\tau) \approx \frac{F_{\tau}(\tau + \Delta\tau) - F_{\tau}(\tau - \Delta\tau)}{2\Delta\tau}, \quad \Delta\tau \ll \tau \quad (13)$$

that gives accurate results in a short amount of time.

First, we investigate the impact of σ and D on the AoA and ToA pdfs, see Figs. 7 and 8.

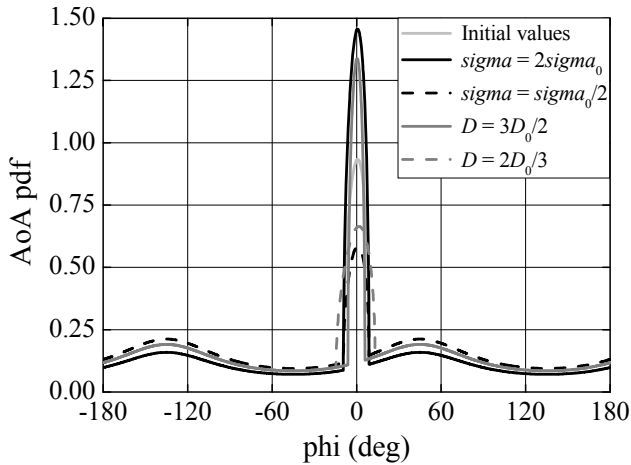


Fig. 7. Impact of σ and D on the AoA pdf.

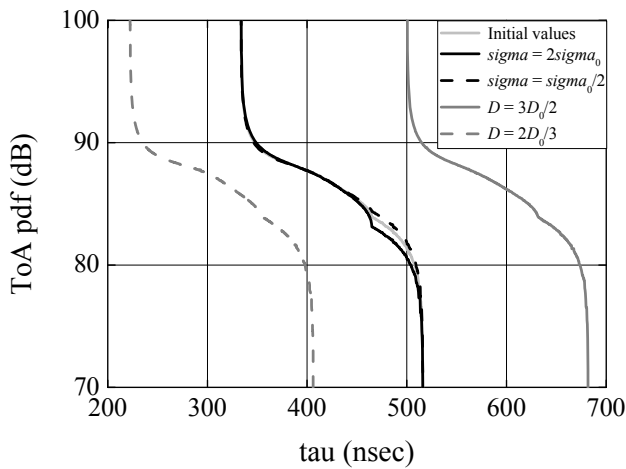


Fig. 8. Impact of σ and D on the ToA pdf.

Fig. 7 shows that the pdf of the angle of arrival of the incoming multipaths increases with D and σ at angles between φ^- and φ^+ ; out of this region, it does not depend on D (at these angles, scattering is due to scatterers at M_1 site only) and decreases slightly with σ . We also notice that φ^\pm depend on D ; see (5). Fig. 8 shows that the curves shift with D along the x -axis; this shift is equal to $(D-D_0)/c$. However, the relative scatterer density does not affect noticeably the ToA pdf.

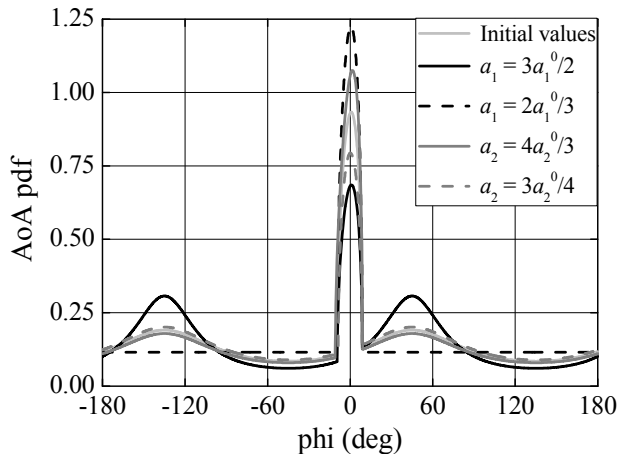


Fig. 9. Impact of the semi-major axes length on the AoA pdf.

Next, in Figs. 9-12 we plot the angle of arrival and time of arrival pdf curves for various lengths of $a_{1,2}$ and $b_{1,2}$. These four figures show that the size of the scattering ellipse around the receiver affects significantly the angular distribution and the delay variation of the received signal. On the contrary, the AoA pdf does not depend on the length of the semi-minor axes of the scattering ellipse at M_2 site while the impact on the channel's temporal characteristics of the scatterers at M_2 is negligible. In both angle of arrival and time of arrival pdf curves, the changes in the semi-major axes lengths affect more noticeably the shape of the curves.

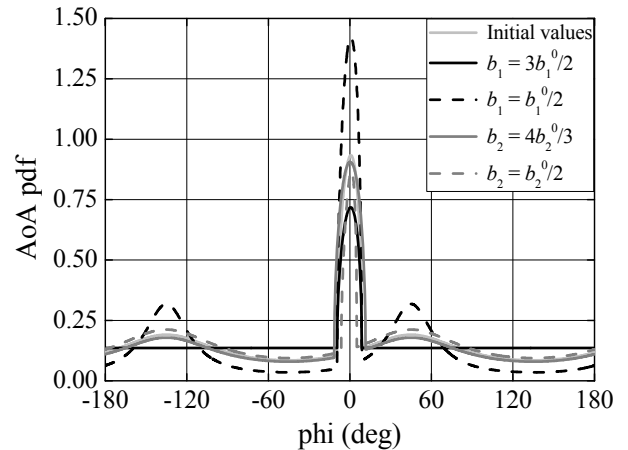


Fig. 10. Impact of the semi-minor axes length on the AoA pdf.

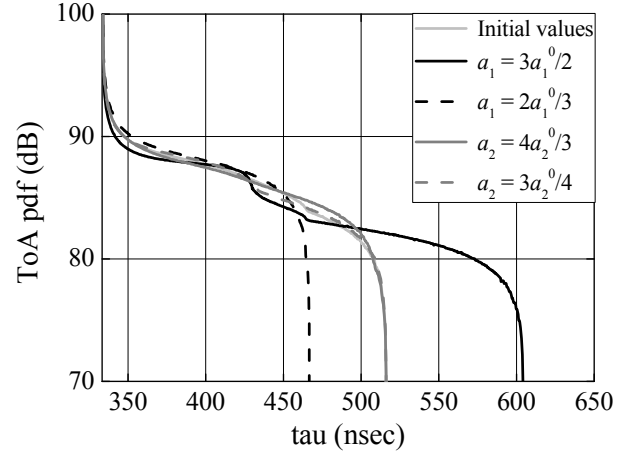


Fig. 11. Impact of a_1 and a_2 on the ToA pdf.

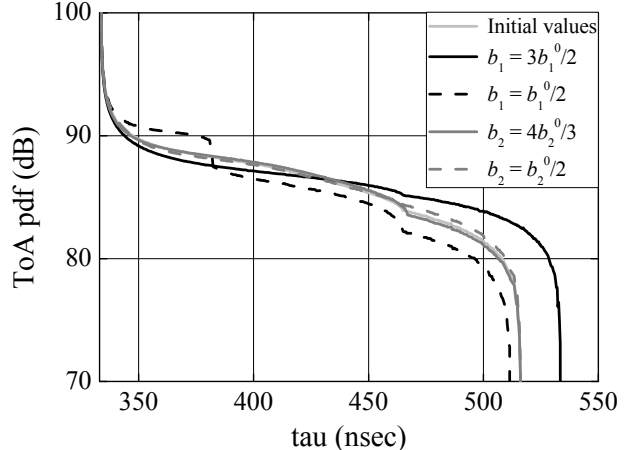


Fig. 12. Impact of b_1 and b_2 on the ToA pdf.

Finally, Fig. 13 shows that the orientation of the scattering ellipse around the receiver affects the AoA pdf curves, esp. at angles outside the range from φ^- to φ^+ ; it also has a strong impact on ToA statistics, see Fig. 14. On the contrary, the ToA pdf does not practically depend on Φ_2 while the orientation of the scattering ellipse at M_2 site has a small impact only on $f_\varphi(\varphi)$ in the range $[\varphi^-, \varphi^+]$.

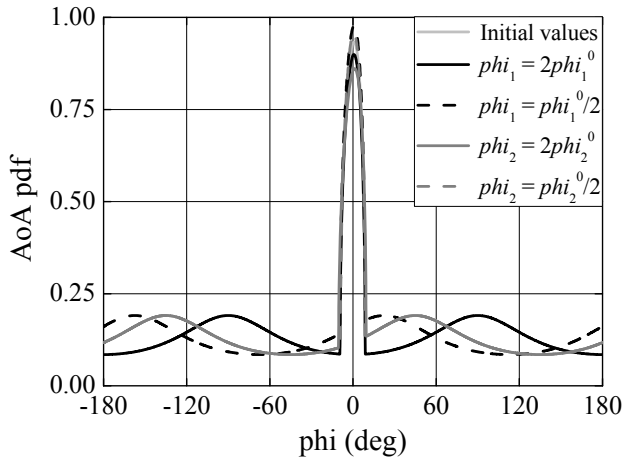


Fig. 13. Impact of the ellipses' orientation on the AoA pdf.

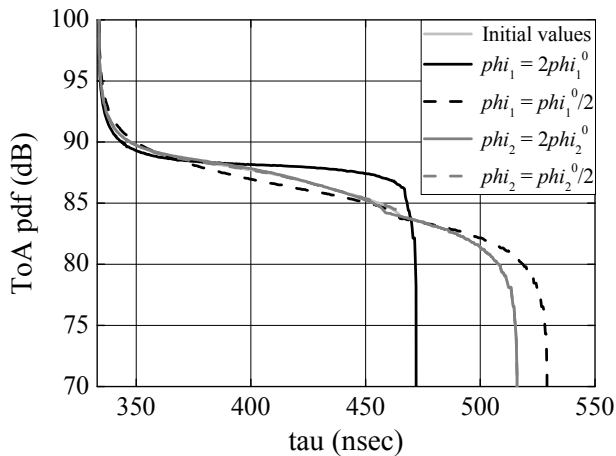


Fig. 14. Impact of the ellipses' orientation on the ToA pdf.

In the aforementioned examples, we have shown that the impact of system parameters on the spatial and temporal channel characteristics is complex. Obviously, this was expected because (7) and (11) depend on seven independent variables (we can normalize the lengths of the scattering ellipses' semi-axes to D). However, our study has shown that some parameters affect significantly the density curves while the impact of others is small. Summarizing the previous results, we have found that both relative scatterer density and separation between mobiles affect the AoA pdf, especially at angles between φ^- and φ^+ , but only D affects the ToA statistics. As far as it concerns the rest of the parameters, we have noticed a strong dependence of AoA and ToA statistics on the geometry of the scattering region around the receiver. On the other hand, only the semi-major axis of the scattering ellipse around the transmitter has a noticeable impact on the AoA pdf while the

delay variation of the received signal does not practically depend on the geometry of this scattering region.

6. Conclusions

In this paper, we proposed a 2-D single bounce geometric scattering model for the spatial and temporal characterization of the M2M channel. In our approach, scatterers are uniformly distributed within ellipses centered at the communicating nodes. We derived a closed-form expression for the AoA pdf and a simple integral formula for the ToA cdf of the received signals. We validated the model through simulations and showed that it is a generalization of popular 2-D channel models. Finally, we explored the relation between the scatterers' distribution and the delay variation and angular distribution of the propagating signal and indicated the significance of the scatterers around the receiver. The proposed model is a useful tool for the study and analysis of channels such as the M2M one when scatterers are distributed around both transmitter and receiver. In fact it is a simplistic model, but offers insight into the channel behavior. The main benefit of this proposal is the simplicity of the expressions that reduces significantly the computational requirements and cost of M2M systems simulations.

References

- [1] WANG, C.-X., CHENG, X., LAURENSEN, D. I. Vehicle-to-vehicle channel modeling and measurements: Recent advances and future challenges. *IEEE Communications Magazine*, 2009, vol. 47, no. 11, p. 96 - 103.
- [2] WIESER, V., PŠENÁK, V. Performance of advanced hybrid link adaptation algorithms in mobile radio channel. *Radioengineering*, 2008, vol. 17, no. 3, p. 81 - 86.
- [3] BALTZIS, K. B. On the effect of channel impairments on VANETs performance. *Radioengineering*, 2010, vol. 19, no. 4, p. 689 - 694.
- [4] BOBAN, M., VINHOZA, T. T. V., FERREIRA, M., BARROS, J., TONGUZ, O. K. Impact of vehicles as obstacles in vehicular ad hoc networks. *IEEE Journal of Selected Areas in Communications*, 2011, vol. 29, no. 1, p. 15 - 28.
- [5] TALHA, B., PÄTZOLD, M. Channel models for mobile-to-mobile cooperative communication systems: A state of the art review. *IEEE Vehicular Technology Magazine*, 2011, vol. 6, no. 2, p. 33 to 43.
- [6] MAURER, J., FÜGEN, T., SCHAFER, T., WIESBECK, W. A new inter-vehicle communications (ivc) channel model. In *Proceedings of the 60th IEEE Vehicular Technology Conference*. Los Angeles (USA), 2004, vol. 1, p. 9 - 13.
- [7] MAURER, J., FÜGEN, T., WIESBECK, W. A ray-optical channel model for vehicular ad-hoc networks. In *Proceedings of the 11th European Wireless Conference*. Nicosia (Cyprus), 2005, p. 1 - 7.
- [8] DIMITRIOU, A. G., BLETSAS, A., POLYCARPOU, A. C., SAHALOS, J. N. Theoretical findings and measurements on planning a UHF RFID system inside a room. *Radioengineering*, 2011, vol. 20, no. 2, p. 387 - 397.

- [9] MALTSEV, A., MASLENNIKOV, R., LOMAYEV, A., SEVASTYANOV, A., KHORYAHEV, A. Statistical channel model for 60 GHz WLAN systems in conference room environment. *Radioengineering*, 2011, vol. 20, no. 2, p. 409 - 422.
- [10] ACOSTA-MARUM, G., INGRAM, M. A. Six time- and frequency-selective empirical channel models for vehicular wireless LANs. *IEEE Vehicular Technology Magazine*, 2007, vol. 2, no. 4, p. 4 - 11.
- [11] SEN, I., MATOLAK, D. W. Vehicle-vehicle channel models for the 5-GHz band. *IEEE Transactions on Intelligent Transportation Systems*, 2008, vol. 9, no. 2, p. 235 - 245.
- [12] RENAUDIN, O., KOLMONEN, V.-M., VAINIKAINEN, P., OESTGES, C. Wideband measurement-based modeling of inter-vehicle channels in the 5 GHz band. In *Proceedings of the 5th European Conference on Antennas and Propagation*. Rome (Italy), 2011, p. 2881 - 2885.
- [13] BALTZIS, K. B. Current issues and trends in wireless channel modeling and simulation. *Recent Patents on Computer Science*, 2009, vol. 2, no. 3, p. 166 - 177.
- [14] CHENG, X., WANG, C.-X., YUAN, Y., LAURENSEN, D. I., GE, X. A novel 3D regular-shaped geometry-based stochastic model for non-isotropic MIMO mobile-to-mobile channels. In *Proceedings of the 72nd IEEE Vehicular Technology Conference*. Ottawa (Canada), 2010, 5 pages, doi:10.1109/VETEFC.2010.5594351.
- [15] PAUL, B. S., HASAN, A., MADHESHIYA, H., BHATTACHARJEE, R. Time and angle of arrival statistics of mobile-to-mobile communication channel employing circular scattering model. *IETE Journal of Research*, 2009, vol. 55, no. 6, p. 275 - 281.
- [16] CHENG, X., WANG, C.-X., LAURENSEN, D. I., SALOUS, S., VASILAKOS, A. V. An adaptive geometry-based stochastic model for non-isotropic MIMO mobile-to-mobile channels. *IEEE Transactions on Wireless Communications*, 2009, vol. 8, no. 9, p. 4824 - 4835.
- [17] PAUL, B. S., BHATTACHARJEE, R. Time and angle of arrival statistics of mobile-to-mobile communication channel employing dual annular strip model. *IETE Journal of Research*, 2010, vol. 56, no. 6, p. 327 - 332.
- [18] TALHA, B., PÄTZOLD, M. A geometrical three-ring-based model for MIMO mobile-to-mobile fading channels in cooperative networks. *EURASIP Journal on Advances in Signal Processing*, 2011, 13 pages, doi:10.1155/2011/892871.
- [19] BALTZIS, K. B., SAHALOS, J. N. A simple 3-D geometric channel model for macrocell mobile communications. *Wireless Personal Communications*, 2009, vol. 51, no. 2, p. 329 - 347.
- [20] PIECHOCKI, R. J., TSOULOS, G. V., MCGEEHAN, J. P. Simple general formula for PDF of angle of arrival in large cell operational environments. *Electronic Letters*, 1998, vol. 34, no. 18, p. 1784 - 1785.
- [21] ERTEL, R. B., REED, J. H. Angle and time of arrival statistics for circular and elliptical scattering models. *IEEE Journal on Selected Areas in Communications*, 1999, vol. 17, no. 11, p. 1829 - 1840.
- [22] POLÁK, L., KRATOCHVÍL, T. Simulation and measurement of the transmission distortions of the digital television DVB-T/H. Part 3: Transmission in fading channels. *Radioengineering*, 2010, vol. 19, no. 4, p. 703 - 711.
- [23] SIMSIM, M. T., KHAN, N. M., RAMER, R., RAPAJIC, P. B. Time of arrival statistics in cellular environments. In *Proceedings of the 63rd IEEE Vehicular Technology Conference*. Melbourne (Australia), 2006, p. 2666 - 2670.
- [24] OLENKO, A. Y., WONG, K. T., NG, E. H.-O. Analytically derived TOA-DOA statistics of uplink/downlink wireless multipaths arisen from scatterers on a hollow-disc around the mobile. *IEEE Antennas and Wireless Propagation Letters*, 2003, vol. 2, p. 345 to 348.

About Author ...

Konstantinos B. BALTZIS received his B.Sc. degree in Physics in 1996, his M.Sc. degree in Communications and Electronics in 1999 and his Ph.D. degree in Communication Engineering in 2005. He belongs to the research staff of the RadioCommunications Laboratory of the Aristotle University of Thessaloniki (AUTH) and he is a teaching staff member in the Program of Postgraduate Studies in Electronic Physics of AUTH. He has published more than thirty papers in international peer-reviewed journals. His current research interests are focused on wireless communications, radio propagation, aperture antennas and microwave systems.